HHS Public Access

Author manuscript

Osteoarthritis Cartilage. Author manuscript; available in PMC 2023 January 01.

Published in final edited form as:

Osteoarthritis Cartilage. 2022 January ; 30(1): 124–136. doi:10.1016/j.joca.2021.09.001.

Systemic Inhibition or Global Deletion of CaMKK2 Protects Against Post-Traumatic Osteoarthritis

Elsa Mével[1,2,@], **Jennifer A. Shutter**[1,2,@], **Xinchun Ding**[1,2,@], **Brett T. Mattingly**[1,2], **Justin N. Williams**[1,2], **Yong Li**[1,2], **Anthony Huls**[1], **Anuradha Valiya Kambrath**[1,2,3], **Stephen B. Trippel**[3], **Diane Wagner**[2,3,4], **Matthew R. Allen**[1,2,3,5], **Regis O'Keefe**[6], **William R. Thompson**[1,2,7], **David B. Burr**[1,2,5], **Uma Sankar**[1,2,#]

[1]Department of Anatomy, Cell Biology and Physiology, Indiana University School of Medicine, Indianapolis, IN 46202, USA

[2]Indiana Center for Musculoskeletal Health, Indiana University School of Medicine, Indianapolis, IN 46202, USA

[3]Department of Orthopaedic Surgery, Indiana University School of Medicine, Indianapolis, IN 46202, USA

[4]Department of Mechanical and Energy Engineering, School of Engineering and Technology, Indianapolis, IN 46202, USA

[5]Department of Medicine, Indiana University School of Medicine, Indianapolis, IN 46202, USA

[6]Department of Orthopaedic Surgery, Washington University School of Medicine, St. Louis, MO 63110, USA

[7]Department of Physical Therapy, School of Health and Rehabilitation Sciences, Indianapolis, IN 46202, USA.

Abstract

Objective: To investigate the role of Ca^{2+}/calmodulin-dependent protein kinase kinase 2 (CaMKK2) in post-traumatic osteoarthritis (PTOA).

[#]**Address correspondences to**: Uma Sankar, Ph.D., 635 Barnhill Drive, MS-5055, Indianapolis, IN 46202 USA. Tel: (317) 274-7870, Fax: (317) 856-5710; usankar@iu.edu.

[@]EM, JAS and XD contributed equally to this study.

Author Contributions

EM, JAS and XD designed and performed experiments, analyzed data, and prepared figures; BTM and JNW performed μCT analysis of SB, statistical analyses and prepared figures, AH performed qRT-PCR experiments; YL performed DMM surgeries and analyzed data; AVK performed imaging, analysis and qRT-PCR; DRW, WRT, SBT, MRA, ROK and DBB provided critical input on data interpretation and edited the manuscript; US conceived and supervised the study, analyzed data, prepared figures and wrote the manuscript.

Conflict of Interest Statement

All authors of this manuscript state that they have no conflict of interest. The authors further state that there are no restrictions on full access for all authors to all raw data, statistical analyses and material used in the study reported in this manuscript.

Methods: Destabilization of the medial meniscus (DMM) or sham surgeries were performed on 10-week-old male wild-type (WT) and *Camkk2*$^{-/-}$ mice. Half of the DMM-WT mice and all other cohorts (n=6/group) received tri-weekly intraperitoneal (i.p.) injections of saline whereas the remaining DMM-WT mice (n=6/group) received i.p. injections of the CaMKK2 inhibitor STO-609 (0.033 mg/kg body weight) thrice a week. Study was terminated at 8- or 12-weeks post-surgery, and knee joints processed for microcomputed tomography imaging followed by histology and immunohistochemistry. Primary articular chondrocytes were isolated from knee joints of 4–6-day-old WT and *Camkk2*$^{-/-}$ mice, and treated with 10 ng/ml interleukin-1β (IL)-1β for 24 or 48 h to investigate gene and protein expression.

Results: CaMKK2 levels and activity became elevated in articular chondrocytes following IL-1β treatment or DMM surgery. Inhibition or absence of CaMKK2 protected against DMM-associated destruction of the cartilage, subchondral bone alterations and synovial inflammation. When challenged with IL-1β, chondrocytes lacking CaMKK2 displayed attenuated inflammation, cartilage catabolism, and resistance to suppression of matrix synthesis. IL-1β-treated CaMKK2-null chondrocytes displayed decreased IL-6 production, activation of signal transducer and activator of transcription 3 (Stat3) and matrix metalloproteinase 13 (MMP13), indicating a potential mechanism for the regulation of inflammatory responses in chondrocytes by CaMKK2.

Conclusions: Our findings reveal a novel function for CaMKK2 in chondrocytes and highlight the potential for its inhibition as an innovative therapeutic strategy in the prevention of PTOA.

Keywords

Osteoarthritis; Ca^{2+}/calmodulin-dependent protein kinase kinase 2 (CaMKK2); destabilization of medial meniscus (DMM); articular chondrocytes; interleukin-1β (IL-1β); IL-6; signal transducer and activator of transcription 3 (Stat3); adenosine monophosphate dependent protein kinase (AMPK)

Introduction

Osteoarthritis (OA) is the leading cause of disability worldwide [1, 2]. OA affects the whole joint, and is characterized by the loss of articular cartilage, subchondral bone (SB) sclerosis, osteophyte formation, synovial inflammation, degeneration of knee ligaments and menisci, and joint capsule hypertrophy [3, 4]. Cartilage injury triggers the release of extracellular matrix (ECM) components such as type II collagen (COL2) and aggrecan (ACAN), leading to the production of inflammatory cytokines including interleukins IL-1β and IL-6, reactive oxygen species such as nitric oxide (NO) and lipid-derived inflammation mediators such as prostaglandin E_2 (PGE_2). These in turn stimulate the chondrocytes to produce matrix-degrading enzymes including matrix metalloproteinases (MMPs) and aggrecanases such as a disintegrin and metalloprotease with thrombospondin motif 5 (ADAMTS5), which further degrade the matrix. Additionally, the inflammatory mediators block anabolic matrix synthesis by chondrocytes [5, 6].

Synovial inflammation, a key hallmark of OA, is marked by macrophage infiltration of the synovium, secretion of IL-1β and thickening of the synovial tissue [7, 8]. This promotes angiogenesis, causing a phenotypic shift in the chondrocytes towards catabolism. Another important feature of OA is SB alterations including subchondral bone plate (SBP)

densification during the later stages of the disease [9, 10]. Successful OA therapies should collectively attenuate or prevent cartilage degradation, synovial inflammation and SB alteration. Unfortunately, there are no treatments against OA, leaving pain therapy and/or joint replacement as the only disease management options.

Calcium/calmodulin-dependent kinase kinase 2 (CaMKK2) is a multifunctional serine/threonine protein kinase that sits at the apex of a signaling cascade that is activated by Ca^{2+}-bound calmodulin (CaM). In addition to its canonical substrates CaMKI and CaMKIV, CaMKK2 phosphorylates adenosine mono phosphate-dependent protein kinase (AMPK) [11, 12], and the CaMKK2/AMPK pathway regulates metabolic responses to stress [13, 14]. *Camkk2*$^{-/-}$ mice are protected from diet-induced obesity, hyperglycemia and insulin resistance as well as macrophage-mediated inflammatory responses[14–16]. Absence of CaMKK2 in macrophages impairs their ability to synthesize inflammatory cytokines in response to Toll like receptor 4 stimulation [15]. *Camkk2*$^{-/-}$ mice display elevated bone mass and strength as they possess fewer osteoclasts and enhanced osteoblasts [17, 18]. As CaMKK2 influences bone remodeling and inflammation, two key mechanisms in early OA, we hypothesized that CaMKK2 plays a role in the pathogenesis of OA. In this study we investigated the role of CaMKK2 in articular cartilage degeneration, synovial inflammation and SB pathology associated with surgically induced OA. Our findings reveal a mechanistic role for CaMKK2 in articular chondrocytes coordinating their inflammatory responses and suggest that its inhibition protects against post-traumatic OA (PTOA).

Method

Mice:

Animal studies were approved by Indiana University School of Medicine (IUSM) Institutional Animal Care and Use Committee (IACUC) and all experiments were performed in compliance with NIH guidelines on the use and care of laboratory and experimental animals. *Camkk2*$^{-/-}$ mice were previously generated through the targeted deletion of exons 2–4 of the mouse *Camkk2* gene [14]. Wild-type (WT) and *Camkk2*$^{-/-}$ mice (both C57BL/6) were housed in the IUSM Laboratory Animal Resource Center (Indianapolis, IN) under 12 h light/dark cycle. Food and water were provided *ad libitum.*

Surgical OA induction:

Mice were randomly assigned to each group. Unilateral destabilization of the medial meniscus (DMM) [19, 20] was performed on 10-week-old male WT (n=24) and *Camkk2*$^{-/-}$ (n=12) mice. Sham surgeries were performed on age and sex-matched WT and *Camkk2*$^{-/-}$ mice (n=12 per cohort). Half of the DMM-WT mice (n=12) received intraperitoneal (i.p.) injections of STO-609 (200 μl of 10 μM solution; 0.033 mg/kg body weight) three times per week (w), starting from the day after the surgery until termination at either 8 or 12 w post-surgery, whereas all the other cohorts received tri-weekly i.p. injections of sterile saline (Supp Fig. 1). STO-609, a selective pharmacological inhibitor of CaMKK2 [21–23] (TOCRIS Bioscience Ellisville, MO, USA), was prepared as reported [18]. Buprenorphine-SR was administered post-surgery. At termination, knee joints were fixed overnight in 4% paraformaldehyde (Polysciences, Warrington, PA, USA) for microcomputed tomography

(μCT) imaging followed by histology and immunohistochemistry (IHC), performed in a blinded manner. Data from the 8 and 12 w post DMM cohorts were analyzed together. There were no outliers in the analyses.

μCT analysis:

SB microarchitecture was analyzed by high-resolution μCT imaging (Skyscan 1172) at a voltage of 60 kV, current at 200 μA and a resolution of 4 μm per pixel. Coronal images of the tibia SB were reconstructed (NRecon software, Kontich, Belgium) and analyzed (CTAn v1.14; Bruker Microct, Kontich, Belgium). The analyzed region of interest covered the whole SB compartment and a total of 200 consecutive images from the tibia plateau was used to measure bone volume per tissue volume (%BV/TV). Fifty consecutive images from the medial tibia plateau in the coronal plane were utilized to measure the SBP thickness (SBP.Th.) (Supp Fig. 2).

Histology and IHC of cartilage and synovium:

Following μCT imaging, whole articulated knee joints were decalcified in 14% EDTA (pH 7.4) and dehydrated before paraffin embedding. Five μm thick serial sections were stained with safranin O fast green (SO) and hematoxylin-eosin (H&E). OA severity was assessed using the OsteoArthritis Research Society International (OARSI) scoring system in a blinded manner on SO-stained serial sections on a scale ranging from 0 to 6 for parameters such as chondrocyte death, hypertrophy, cluster, loss of SO staining, surface and bone alterations [24]. Synovitis was also evaluated using the OARSI system [25–27]. Scoring was performed at four different section levels of the joint and the highest score was recorded per published guidelines [25]. IHC was performed with primary antibodies indicated in Table 1, and counterstained with Gill No. 1 Hematoxylin or Methyl Green (Millipore Sigma, Burlington, MA). Images captured using a Leica DMi8 microscope were processed with Leica LAS-X software (Leica CM1950, Wetzlar, Germany), and quantified by counting immunopositive and total cells within articular cartilage from 4 regions of interest per sample using ImageJ (NIH, USA).

Primary murine articular chondrocyte (iMAC) isolation and culture:

iMACs were isolated as previously described [28] from knee joints of 4–6 day-old WT and *Camkk2*$^{-/-}$ mice. Cartilage, devoid of epiphyseal tissues, was pooled from 6–8 pups per genotype, minced and sequentially digested with two different concentrations of collagenase D (Millipore Sigma), 2.5 mg/ml for 1.5 h, followed by 0.5 mg/ml overnight, at 37°C with shaking. P0 chondrocytes were plated on 6-well dishes at a density of 75,000 cells/cm^2 in Dulbecco's Modified Eagle's Medium (DMEM 4.5 g/L glucose) (Thermo Fisher) supplemented with 10% Fetal bovine serum (FBS) and 1% penicillin/streptomycin (Thermo Fisher) for 24 h. Cells were serum starved for 12 h for synchronization, and then released into full media containing 10% FBS before treating with 10 ng/ml human recombinant IL-1β (Millipore Sigma) for 24–48 h or as indicated.

ELISA:

ELISAs were performed using commercially available kits for assessing levels of NO, PGE_2 and IL-6 (Cat# 760871, 514010 and 583371 from Cayman Chemical, Ann Arbor, MI), and glycosaminoglycan (GAG; Cat# 280560-N - Amsbio Abingdon, UK) from freshly frozen culture supernatants harvested from P0 chondrocytes treated with or without 10 mg/ml IL-1β for 48 h, as indicated above. Fifty to 100 μl of culture supernatants diluted per kit instructions was used for the assays.

Quantitative reverse transcription polymerase chain reaction (qRT-PCR):

Total RNA was isolated from P0 iMACs treated with or without 10 ng/ml IL-1β for 48 h, using RNAqueous 4-PCR kit, and cDNA was generated using High Capacity cDNA Reverse Transcription Kit (both from Thermo Fisher). QRT-PCR was performed using iTaq™ Universal SYBR® Green Supermix on the CFX Connect™ Real-Time system (Bio-Rad Laboratories, Hercules, CA, USA). PCR primers (Table 2) were synthesized by Integrated DNA technologies (Coralville, IA, USA). mRNA levels were normalized to β-actin and quantified using the Livak method [29].

Immunoblotting:

P0 iMACs were treated with or without 10 ng/ml IL-1β for time points indicated in Figures 1 and 6. Equal amount of protein lysates was fractionated under denaturing conditions on SDS-PAGE and transferred onto Immobilon-P membranes (Millipore Sigma). Blocking, primary and secondary antibody incubations were performed in Tris-buffered saline (TBS) containing 5% non-fat dry milk. Washes were performed in TBS with Tween-20 (0.1%, v/v, Millipore Sigma). Membranes were probed with primary antibodies (Table 1) and horseradish peroxidase-conjugated secondary antibodies (Jackson Immunoresearch Laboratories, West Grove, PA, USA). The target proteins were visualized with chemiluminescence substrate (Bio-Rad) using a ChemiDox MP Image System (Bio-Rad), and band densities quantified using Image lab (Bio-Rad).

Immunoprecipitation and CaMKK2 activity assay:

P0 WT and *Camkk2*$^{-/-}$ chondrocyte treated with or without IL-1β (10ng/ml) for 24 h, were harvested and placed into iced tween lysis buffer (25 mM Hepes (pH 7.5), 50 mM NaCI, 25 mM NaH2PO4, 0.5% Tween 20, 10% glycerol, 1 mM dTT, 10 mM β-glycerophosphate, 2 mM EGTA, 2 mM EDTA, 25 mM NaF, 1 mM sodium vanadate, 1 mM PMSF, 1 mg/ml aprotinin, 1 mg/ml leupeptin, 10 mg/ml pefabloc, and 100 nM okadaic acid), sonicated on ice, centrifuged 14000 rpm for 30 min at 4°C. About 500 μg total protein was precleared with 5 μl of protein G mag Sepharose (Millipore Sigma), and incubated with 5 μg rabbit IgG or rabbit anti-CaMKK2-NT antibody (US Biological) and 5 μl protein G mag Sepharose beads overnight at 4°C. Next day, the beads were spun down, washed, resuspended in 100 μl kinase buffer (20 mM Hepes pH 7.5, 10 mM $MgCl_2$, 0.05 mM ATP, 600 nM calmodulin, 5 mM $CaCl_2$, and 5 ug/ml recombinant hCaMKIV (NBP1–78878 Novus Biologicals, Centennial, CO)), and incubated at 30°C for 30 min with gentle shaking [30–32]. Two μl of kinase assays were resolved by SDS-PAGE and immunoblotted for CaMKK2, and phospho and total CaMKIV (Table 1).

Statistics:

Sample size of n=6 mice per group per time point was selected for in vivo DMM experiments to allows us to detect a mean difference of 1.8 SD vs. zero difference for cartilage parameters (OARSI score) with 80% power at type I error level 0.05 using Student's t-test. Statistical analyses were performed using the GraphPad Prism software (GraphPad Software, San Diego, CA). Normality assumptions were evaluated using histograms and QQ plots which suggested no apparent violations of normality. Consequently, ordinary one-way ANOVA were performed followed by Tukey's multiple comparison tests to compare the mean of each group to that of every other group[33]. Differences with a p-value < 0.05 were deemed significant.

Results

Inflammatory cues elevate CaMKK2 levels and activity in articular chondrocytes

CaMKK2 is expressed in iMACs and its levels significantly increased within 15 min of treatment with IL-1β, and became 7.5-fold higher than control cells by 24–48 h of treatment (Fig. 1A). We next wanted to understand if the enhanced CaMKK2 translated to increased activity. CaMKK2 uniquely possesses substantial Ca^{2+}/CaM-independent activity due to multi-site phosphorylation at its N-terminus by cyclin-dependent kinase 5 and glycogen synthase kinase 3 [32, 34, 35]. Upon Ca^{2+}/CaM binding, CaMKK2 autophosphorylates Thr482 within its autoinhibitory region, enhancing its autonomous activity [32]. Unfortunately, no reliable antibodies are commercially available to evaluate the phosphorylation status of CaMKK2 at any of these sites. Therefore, we immunoprecipitated CaMKK2 from iMACs treated with or without IL-1β for 24 h and incubated the immunocomplexes with recombinant CaMKIV, a canonical CaMKK2 substrate [12]. Indeed, CaMKK2 immunoprecipitates from IL-1β-treated WT iMACs possessed elevated levels of the kinase, and they phosphorylated recombinant CaMKIV at higher levels compared to those from control WT or *Camkk2*$^{-/-}$ iMACs (Fig. 1B).

CaMKK2 levels were significantly elevated in articular cartilage in vivo following DMM surgery (Fig. 1C–D, Supp. Fig. 3). Phosphorylated (p)CaMKIV was also elevated 4-fold in articular chondrocytes following DMM surgery, and this was suppressed in WT-DMM mice that were treated with STO-609, an inhibitor of CaMKK2 activity but not its expression (Fig. 1C, 1E). Conversely, pCaMKIV levels remained unchanged in the articular cartilage of *Camkk2*$^{-/-}$ mice regardless of surgery (Fig. 1C, 1E). Thus, CaMKK2 levels and activity are upregulated in chondrocytes by inflammatory signals.

Loss or inhibition of CaMKK2 protects from cartilage destruction, synovitis and SB sclerosis associated with PTOA

We hypothesized that CaMKK2 plays a role in coordinating cartilage inflammatory responses to joint injury, and that its absence or inhibition will protect from surgically induced PTOA. To test this, we performed sham or DMM surgeries in 10 w old male WT and *Camkk2*$^{-/-}$ mice, treated half of the WT-DMM mice with the CaMKK2 inhibitor STO-609 [22, 23] and the remaining cohorts with saline for 8- or 12-weeks post-surgery (Supp. Fig. 1). Cartilage pathology associated with DMM surgery was observed in WT-DMM-

saline knees, first as focal discontinuity of the cartilage superficial zone at 8 w post-DMM (Supp. Fig. 4), and then as a significant erosion of the articular cartilage at 12 w post-surgery (Fig. 2A). OARSI scoring revealed a significantly elevated (4–6-fold higher) degeneration of the articular cartilage following surgery (Fig. 2B). In contrast, WT-DMM mice treated with STO-609 (WT-DMM-STO-609), displayed minor abrasion to the cartilage superficial zone, with some loss of proteoglycan content (Fig. 2A, Supp. Fig. 4), but no apparent loss of the articular cartilage matrix, with an OARSI score 2.7-fold lower than WT-DMM-saline but not significantly different from those in WT-sham mice at both timepoints examined (Fig. 2B). We found no damage to the articular cartilage damage and no significant differences in OARSI scoring between *Camkk2*$^{-/-}$ sham and *Camkk2*$^{-/-}$ DMM mice (Fig. 2A–2B, Supp. Fig. 4). These data indicate that blocking CaMKK2 prevents DMM-induced cartilage damage.

Compared to WT-sham, WT-DMM-saline knee joints displayed synovial membrane hyperplasia (Fig. 3A and Supp. Fig. 5). In contrast, only a mild thickening of the synovial membrane with no increase in cellularity was observed in WT-DMM-STO-609 knee joints (Fig. 3A). Synovial histopathology grading revealed a 3- and 6-fold increase in synovitis-severity at 8 and 12 w post-surgery respectively in WT-DMM-saline compared to WT-sham, which was significantly inhibited with STO-609 treatment (Fig 3B). Furthermore, DMM did not induce synovitis in *Camkk2*$^{-/-}$ mice (Fig. 3A–3B). Thus, the inhibition or loss of CaMKK2 significantly abrogates synovial inflammation associated with PTOA.

Injury-associated abnormal joint loading induces mechanical stress that results in SB alterations, which manifests as sclerosis in late OA [8, 9]. Analysis of μCT images revealed significantly higher SB % BV/TV and SBP thickness at 8 and 12 w post-DMM in WT-DMM-saline mice compared to WT-sham, indicating DMM-associated SB densification, and treatment with STO-609 attenuated this increase (Fig. 4A–4C). Sham and DMM-operated *Camkk2*$^{-/-}$ mice possessed similar SB %BV/TV and SBP thickness, indicating the absence of OA-associated SB pathology in *Camkk2*$^{-/-}$ mice (Fig. 4B–4C).

Absence of CaMKK2 attenuates inflammatory and catabolic responses, and protects cartilage anabolic marker expression in articular chondrocytes

Macrophages in the inflamed synovium produce IL-1β and IL-6 which stimulate the release of MMPs and aggrecanases by chondrocytes [36–38]. To understand if the inhibition or loss of CaMKK2 suppressed these cellular mechanisms, we examined the levels of the pan-macrophage marker F4/80 [39] and MMP-13 in sham and DMM-operated knees from WT and *Camkk2*$^{-/-}$ mice. WT-DMM-saline knees possessed enhanced numbers of F4/80-positive cells in the synovial membrane compared to WT-sham whereas treatment with STO-609 or the absence of CaMKK2 *(Camkk2*$^{-/-}$ mice) significantly attenuated this response (Supp. Fig. 6A). Further, MMP13 levels in articular chondrocytes were significantly elevated in WT-DMM-saline knees but not in WT-DMM-STO-609 or *Camkk2*$^{-/-}$-DMM knees (Supp. Fig. 6B). Conversely, COL2 content in articular chondrocytes was reduced by 2.9-fold in WT-DMM-saline knees compared to WT-sham, and treatment with STO-609 protected against this loss. Notably, DMM surgery did not affect COL2 content in *Camkk2*$^{-/-}$ articular cartilage (Supp. Fig. 6C).

Next, we stimulated WT and *Camkk2*$^{-/-}$ iMACs with 10 ng/ml of IL-1β for 48 h and evaluated secreted NO, PGE_2 and IL-6 protein in the media as well as *Inos, Cox2* and *Il-6* mRNA (Fig. 5A–Ai). Consistent with previous reports [40, 41], we observed enhanced levels of NO (18-fold), PGE_2 (17-fold) and IL-6 (93-fold) secreted into the media by IL-1β-stimulated WT iMACs (Fig. 5A). In contrast, *Camkk2*$^{-/-}$ iMACs treated with IL-1β secreted significantly lower levels of inflammatory molecules into the media. Further, whereas IL-1β elicited a robust elevation in *Inos, Cox2* and *Il-6* mRNA in WT iMACs, the response was attenuated in IL-1β-stimulated *Camkk2*$^{-/-}$ iMACs (Fig. 5Ai). In particular, the absence of CaMKK2 in iMACs significantly impaired IL-1β-mediated upregulation of IL-6 mRNA and protein (Fig. 5A–Ai). Furthermore, whereas IL-1β stimulated a marked upregulation of *Mmp2, Mmp9, Mmp13* and *Adamts5* in both genotypes, the level of upregulation of *Mmp2, Mmp13* and *Adamts5* was significantly lower while that of *MMP-9* trended lower (p=0.10) in *Camkk2*$^{-/-}$ iMACs than WT (Fig. 5B).

Further, IL-1β induced a significant downregulation of *Acan* and cartilage oligomeric matrix protein *(Comp* or thrombospondin-5) in WT and *Camkk2*$^{-/-}$ iMACs but the mutant cells still possessed 3-fold higher levels of *Acan* (p=0.06) and 4-fold higher *Comp* mRNA compared to WT after 48 h of IL-1β treatment (Fig. 5C). Interestingly, *Col2a1* transcripts were significantly upregulated in IL-1β-treated *Camkk2*$^{-/-}$ iMACs, 2.5-fold higher than untreated *Camkk2*$^{-/-}$ iMACs and 5-fold higher than IL-1β-treated WT iMACs (Fig. 5C). Furthermore, whereas IL-1β potentiated a significant reduction in glycosaminoglycan (GAG) content in WT iMACs, it failed to do so in *Camkk2*$^{-/-}$ iMACs. Notably, GAG content in IL-1β-treated *Camkk2*$^{-/-}$ iMACs was significantly higher than in IL-1β-treated WT iMACs (Figure 5C). Thus, the absence of CaMKK2 attenuates IL-1β-mediated inflammatory and catabolic responses while protecting the chondrocytes from its anti-anabolic effects.

Stat3 and AMPK activation by IL-1β are attenuated in CaMKK2 null chondrocytes

IL-1β-treated *Camkk2*$^{-/-}$ iMACs are impaired in their ability to upregulate IL-6 (Fig. 5A–Ai), and IL-6 triggers cartilage catabolic effects via MMP13 and ADAMTS-5 through the activation of Stat3 in chondrocytes [42–45]. Therefore, we examined Stat3 activation by IL-1β in WT and *Camkk2*$^{-/-}$ iMACs, and found lower phospho (p) Stat3 levels in IL-1β treated *Camkk2*$^{-/-}$ iMACs compared to WT (Fig. 6A, 6D). Moreover, levels of MMP-13, a target of the IL-6-Stat3 pathway in chondrocytes [45], were significantly lower in naïve and IL-1β-treated *Camkk2*$^{-/-}$ iMACs compared to WT (Figs 6A, 6E).

AMPK, a direct target of CaMKK2 and a key regulator of cellular energy homeostasis, plays an important role in protecting chondrocytes against inflammation [11, 46–50]. Surprisingly, we found pAMPK levels to be significantly elevated by IL-1β in WT iMACs at 1- and 2-days of treatment. In contrast, the levels of pAMPK were significantly lower regardless of IL-1β treatment in *Camkk2*$^{-/-}$ iMACs than WT. Specifically, pAMPK levels in naïve *Camkk2*$^{-/-}$ iMACs were 4-fold lower at basal conditions whereas they were 2.6-fold and 7.1-fold lower at 1- and 2-days of IL-1β treatment respectively, compared to those in WT iMACs (Fig. 6B, 6F). Together, these data indicate that CaMKK2 plays a key role in basal AMPK phosphorylation in chondrocytes as well as its acute activation by IL-1β.

IL-1β activates several signaling pathways in chondrocytes including extracellular signal-regulated kinase (ERK)1/2, p38 mitogen-activated protein kinase (MAPK) and p65 (Rel1/NF-κB) [51]. Therefore, we examined whether the activation of these signaling pathways by IL-1β is altered in CaMKK2 null chondrocytes, and found them to be similarly activated in WT and *Camkk2*$^{-/-}$ iMACs (Fig. 6C, 6H–6J). We also observed p-S6K/mTOR, a kinase with roles in OA pathogenesis that is inhibited by AMPK [52, 53], to be similarly upregulated by IL-1β in WT and *Camkk2*$^{-/-}$ iMACs (Fig. 6C, 6K). Thus, the activation of ERK, p38 MAPK, p65 (Rel1/NF-κB) and S6K/mTOR by IL-1β is not regulated by CaMKK2.

Discussion

Using a mouse model of PTOA, we show that the absence or inhibition of CaMKK2 protects against OA pathogenesis. Specifically, trauma-induced damage of the articular cartilage, synovial membrane hyperplasia, macrophage infiltration of the synovium, and OA-associated SB sclerosis were all significantly abrogated when the presence of CaMKK2 or its activity was blocked. Articular chondrocytes express CaMKK2 and inflammatory cues such as joint injury or IL-1β elevate its levels and activity. In the absence of CaMKK2, IL-1β-mediated production of inflammation mediators such as IL-6, NO, and PGE_2 as well as proteolytic enzymes such as MMP13 and ADAMTS5 by chondrocytes was significantly attenuated. Most notably, this was coupled with a protection from IL-1β-mediated suppression of matrix synthesis in *Camkk2*$^{-/-}$ iMACs. Specifically, our observation of *Col2a1* mRNA being significantly increased (by 2.3-fold) in *Camkk2*$^{-/-}$ iMACs treated for 48 h with IL-1β is interesting (Fig. 5C). The exact mechanism contributing to the acute upregulation *Col2a1* gene expression in IL-1β-treated *Camkk2*$^{-/-}$ iMACs is unknown. Previous studies indicate downregulation of the high mobility group box containing transcription factor Sox9 and COL2 through an IL-6-JAK/Stat-dependent mechanism in primary bovine articular chondrocytes [54]. Sox-9 is the master regulator of chondrocyte differentiation and is required for the expression of *Col2a1*[55, 56]. Indeed, stimulation of the IL-6-Stat3 pathway by IL-1β is downregulated in *Camkk2*$^{-/-}$ chondrocytes, suggesting a key role for CaMKK2 in inflamed chondrocytes. Exactly how CaMKK2 is involved in this mechanism is unclear, though IL-6-CaMKK2 cross-talk has been reported in other cell types [57]. Based on these data, we posit that the ability of IL-1β-IL-6-pStat3 to suppress Sox-9 and *Col2a1* in iMACs is blocked in the absence of CaMKK2.

Synovial inflammation in OA is milder than in classic inflammatory diseases such as rheumatoid arthritis. Still, injury associated secretion of inflammatory chemokines by chondrocytes attracts macrophages to infiltrate the synovial membrane and potentiate inflammation, which triggers pain [6, 38]. DMM-induced synovial inflammation is abrogated in *Camkk2*$^{-/-}$ and STO-609-treated WT mice. We propose that the suppression of inflammatory responses in CaMKK2-deficient chondrocytes eliminates the source of the chemokine response attracting immune cells to the synovium, and that this protects against synovial inflammation. Conversely, since CaMKK2 possesses cell-autonomous roles in macrophages [15] and its levels in synovial macrophages are elevated following DMM surgery in WT mice (data not shown), its absence specifically in macrophages could influence the overall OA pathology. It is important to decipher in future studies whether protection from

OA-associated synovial pathology in the absence of CaMKK2 stems from a primary effect on chondrocytes or macrophages or both.

DMM-induced SB sclerosis or SBP thickness was not observed in WT mice treated with STO-609 or in *Camkk2*$^{-/-}$ mice, indicating that the inhibition or loss of the kinase protects against SB alterations associated with OA. CaMKK2 null mice, regardless of surgery, possessed higher SB % BV/TV and SBP thickness compared to WT, as reported for long bones in previous studies [17, 18]. Nevertheless, DMM surgery did not alter the SB or SBP in *Camkk2*$^{-/-}$ mice. CaMKK2 has roles in bone remodeling [17, 18, 58], and it is possible that the protection from OA-induced SB alterations observed in *Camkk2*$^{-/-}$ mice are due to its cell-autonomous effects in bone cells. However, we cannot also rule out the possibility that the primary effect stems from a cell-intrinsic role of the kinase in chondrocytes, which abrogates injury-initiated SB alterations.

Absence of CaMKK2 resulted in lower basal AMPK phosphorylation in iMACs and its muted activation by IL-1β. These results are interesting given the role played by AMPK in coordinating metabolic regulation of inflammatory responses in chondrocytes [48]. The prototypic AMPK kinase (AMPKK) is liver kinase B1 (LKB1), which phosphorylates the catalytic subunit AMPKα on Thr-172 in the activation loop, upon activation by increased AMP:ATP ratio. In some cell types, CaMKK2 also serves as an AMPKK, phosphorylating AMPKα on the same Thr-172, but in response to increases in intracellular Ca^{2+}.However, in contrast to the LKB1-heterotrimeric AMPKα/β/γ complex, the CaMKK2-AMPK complex lacks the AMPKγ-subunit which usually binds to AMP. In this case, CaMKK2 substitutes for AMPKγ to stabilize AMPKα/β and confer Ca^{2+}/CaM sensitivity to the complex [12, 14]. Since IL-1β-induced acute (24 and 48 h post-treatment) activation of AMPK is downregulated in *Camkk2*$^{-/-}$ iMACs, we posit that the stimulation of iMACs by IL-1β triggers transient increases in intracellular Ca^{2+}, which results in the complexing of CaMKK2-AMPKα/β rather than LKB1- AMPKα/β/γ. IL-1β-mediated acute activation of AMPK in chondrocytes has been reported [59], although the exact role of this mechanism is unclear. In summary, our findings highlight a role for CaMKK2 in regulating inflammatory and catabolic responses in chondrocytes by promoting the expression of IL-6 and other inflammatory mediators and as well as matrix-degrading enzymes such as MMP13 through a Stat3-mediated mechanism. Blocking CaMKK2 helps maintain matrix synthesis by chondrocytes when exposed to inflammatory cytokines. Taken together, the data presented here identify CaMKK2 as an effective therapeutic target in the treatment of PTOA, a disease with no effective disease-modifying treatments.

Supplementary Material

Refer to Web version on PubMed Central for supplementary material.

Acknowledgments

The authors thank Dr. Ziyue Liu, Associate Professor of Biostatistics & Health Data Sciences, IUSM for help with statistical analysis, Dr. Keith W. Condon for help with histology and guidance on immunohistochemistry, and Dr. Lilian Plotkin, Drew M. Brown and the staff at the Musculoskeletal Histology Core Facility of the Indiana Center for Musculoskeletal Health and the Bone and Body Composition Core of the Indiana Clinical Translational Sciences Institute (CTSI) for histology.

Funding Source

Research reported in this manuscript was supported by the National Institute Of Arthritis And Musculoskeletal And Skin Diseases of the National Institutes of Health under Award Numbers R01AR076477 and R01AR068332 (both to US); and an Indiana Center for Musculoskeletal Heath (ICMH) Pilot Grant Award to US. This work was also supported by funds from the Indiana Clinical and Translational Sciences Institute funded in part by Award Number UL1TR001108 from the National Institutes of Health, National Center for Advancing Translational Sciences, Clinical and Translational Sciences Award to EM. The 1172 μCT system was supported by an S10 grant (S10-RR023710) to MRA. JN was supported through a Comprehensive Musculoskeletal T32 Training Program from NIAMS/NIH (AR065971). JAS is supported by the Moenkhaus fellowship from the Department of Anatomy, Cell Biology & Physiology at IUSM. The study sponsors were not involved in any aspects of this study including study design, collection, analysis and interpretation of data; or in the writing of the manuscript, and in the decision to submit the manuscript for publication. The content is solely the responsibility of the authors and does not necessarily represent the official views of the National Institutes of Health.

References

1. Plotnikoff R, Karunamuni N, Lytvyak E, Penfold C, Schopflocher D, Imayama I, et al. Osteoarthritis prevalence and modifiable factors: a population study. BMC Public Health. 2015; 15:1195. Epub 2015/12/02. doi: 10.1186/s12889-015-2529-0. [PubMed: 26619838]
2. Nuesch E, Dieppe P, Reichenbach S, Williams S, Iff S, Juni P. All cause and disease specific mortality in patients with knee or hip osteoarthritis: population based cohort study. BMJ. 2011;342(mar08 2):d1165-d. doi: 10.1136/bmj.d1165. [PubMed: 21385807]
3. Loeser RF, Goldring SR, Scanzello CR, Goldring MB. Osteoarthritis: A disease of the joint as an organ. Arthritis & Rheumatism. 2012;64(6):1697–707. doi: 10.1002/art.34453. [PubMed: 22392533]
4. Deveza LA, Loeser RF. Is osteoarthritis one disease or a collection of many? Rheumatology (Oxford). 2017. Epub 2017/12/22. doi: 10.1093/rheumatology/kex417.
5. Chen D, Shen J, Zhao W, Wang T, Han L, Hamilton JL, et al. Osteoarthritis: toward a comprehensive understanding of pathological mechanism. Bone Research. 2017;5:16044. doi: 10.1038/boneres.2016.44. [PubMed: 28149655]
6. Loeser RF. Molecular mechanisms of cartilage destruction in osteoarthritis. J Musculoskelet Neuronal Interact. 2008;8(4):303–6. Epub 2009/01/17. [PubMed: 19147949]
7. Benito MJ, Veale DJ, FitzGerald O, van den Berg WB, Bresnihan B. Synovial tissue inflammation in early and late osteoarthritis. Ann Rheum Dis. 2005;64(9):1263–7. doi: 10.1136/ard.2004.025270. [PubMed: 15731292]
8. Mathiessen A, Conaghan PG. Synovitis in osteoarthritis: current understanding with therapeutic implications. Arthritis Research & Therapy. 2017;19(1). doi: 10.1186/s13075-017-1229-9.
9. Burr DB, Gallant MA. Bone remodelling in osteoarthritis. Nature Reviews Rheumatology. 2012;8(11):665–73. doi: 10.1038/nrrheum.2012.130. [PubMed: 22868925]
10. Burr DB, Utreja A. Editorial: Wnt Signaling Related to Subchondral Bone Density and Cartilage Degradation in Osteoarthritis. Arthritis & rheumatology (Hoboken, NJ). 2018;70(2):157–61. doi: 10.1002/art.40382.
11. Hurley RL, Anderson KA, Franzone JM, Kemp BE, Means AR, Witters LA. The Ca2+/calmodulin-dependent protein kinase kinases are AMP-activated protein kinase kinases. The Journal of biological chemistry. 2005;280(32):29060–6. Epub 2005/06/28. doi: M503824200 [pii] 10.1074/jbc.M503824200. [PubMed: 15980064]
12. Means AR. The Year in Basic Science: calmodulin kinase cascades. Molecular endocrinology. 2008;22(12):2759–65. Epub 2008/10/11. doi: 10.1210/me.2008-0312. [PubMed: 18845671]
13. Anderson KA, Lin F, Ribar TJ, Stevens RD, Muehlbauer MJ, Newgard CB, et al. Deletion of CaMKK2 from the liver lowers blood glucose and improves whole-body glucose tolerance in the mouse. Mol Endocrinol. 2012;26(2):281–91. Epub 2012/01/14. doi: 10.1210/me.2011-1299. [PubMed: 22240810]
14. Anderson KA, Ribar TJ, Lin F, Noeldner PK, Green MF, Muehlbauer MJ, et al. Hypothalamic CaMKK2 Contributes to the Regulation of Energy Balance. Cell Metabolism. 2008;7(5):377–88. [PubMed: 18460329]

15. Racioppi L, Noeldner PK, Lin F, Arvai S, Means AR. Calcium/Calmodulin-dependent Protein Kinase Kinase 2 Regulates Macrophage-mediated Inflammatory Responses. Journal of Biological Chemistry. 2012;287(14):11579–91. doi: 10.1074/jbc.m111.336032.

16. Marcelo KL, Means AR, York B. The Ca(2+)/Calmodulin/CaMKK2 Axis: Nature's Metabolic CaMshaft. Trends in endocrinology and metabolism: TEM. 2016;27(10):706–18. Epub 2016/07/28. doi: 10.1016/j.tem.2016.06.001. [PubMed: 27449752]

17. Pritchard ZJ, Cary RL, Yang C, Novack DV, Voor MJ, Sankar U. Inhibition of CaMKK2 reverses age-associated decline in bone mass. Bone. 2015;75:120–7. doi: 10.1016/j.bone.2015.01.021. [PubMed: 25724145]

18. Cary RL, Waddell S, Racioppi L, Long F, Novack DV, Voor MJ, et al. Inhibition of Ca2+/Calmodulin-Dependent Protein Kinase Kinase 2 Stimulates Osteoblast Formation and Inhibits Osteoclast Differentiation. Journal of Bone and Mineral Research. 2013;28(7):1599–610. doi: 10.1002/jbmr.1890. [PubMed: 23408651]

19. Glasson SS, Blanchet TJ, Morris EA. The surgical destabilization of the medial meniscus (DMM) model of osteoarthritis in the 129/SvEv mouse. Osteoarthritis and cartilage. 2007;15(9):1061–9. doi: 10.1016/j.joca.2007.03.006. [PubMed: 17470400]

20. Mevel E, Merceron C, Vinatier C, Krisa S, Richard T, Masson M, et al. Olive and grape seed extract prevents post-traumatic osteoarthritis damages and exhibits in vitro anti IL-1beta activities before and after oral consumption. Sci Rep. 2016;6:33527. doi: 10.1038/srep33527. [PubMed: 27640363]

21. Kukimoto-Niino M, Yoshikawa S, Takagi T, Ohsawa N, Tomabechi Y, Terada T, et al. Crystal Structure of the Ca2+/Calmodulin-dependent Protein Kinase Kinase in Complex with the Inhibitor STO-609. Journal of Biological Chemistry. 2011;286(25):22570–9. doi: 10.1074/jbc.M111.251710.

22. Tokumitsu H, Inuzuka H, Ishikawa Y, Ikeda M, Saji I, Kobayashi R. STO-609, a specific inhibitor of the Ca(2+)/calmodulin-dependent protein kinase kinase. The Journal of biological chemistry. 2002;277(18):15813–8. Epub 2002/02/28. doi: 10.1074/jbc.M201075200. [PubMed: 11867640]

23. York B, Li F, Lin F, Marcelo KL, Mao J, Dean A, et al. Pharmacological inhibition of CaMKK2 with the selective antagonist STO-609 regresses NAFLD. Sci Rep. 2017;7(1):11793. doi: 10.1038/s41598-017-12139-3. [PubMed: 28924233]

24. Pritzker KPH, Gay S, Jimenez SA, Ostergaard K, Pelletier JP, Revell PA, et al. Osteoarthritis cartilage histopathology: grading and staging. Osteoarthritis and cartilage. 2006;14(1):13–29. doi: 10.1016/j.joca.2005.07.014. [PubMed: 16242352]

25. Glasson SS, Chambers MG, Van Den Berg WB, Little CB. The OARSI histopathology initiative – recommendations for histological assessments of osteoarthritis in the mouse. Osteoarthritis and cartilage. 2010;18:S17–S23. doi: 10.1016/j.joca.2010.05.025.

26. Kraus VB, Huebner JL, DeGroot J, Bendele A. The OARSI histopathology initiative – recommendations for histological assessments of osteoarthritis in the guinea pig. Osteoarthritis and cartilage. 2010;18:S35–S52. doi: 10.1016/j.joca.2010.04.015. [PubMed: 20864022]

27. Pelletier JP, Martel-Pelletier J, Ghandur-Mnaymneh L, Howell DS, Woessner JF Jr. Role of synovial membrane inflammation in cartilage matrix breakdown in the Pond-Nuki dog model of osteoarthritis. Arthritis Rheum. 1985;28(5):554–61. Epub 1985/05/01. doi: 10.1002/art.1780280515. [PubMed: 2988573]

28. Gosset M, Berenbaum F, Thirion S, Jacques C. Primary culture and phenotyping of murine chondrocytes. Nature Protocols. 2008;3(8):1253–60. doi: 10.1038/nprot.2008.95. [PubMed: 18714293]

29. Livak KJ, Schmittgen TD. Analysis of relative gene expression data using real-time quantitative PCR and the 2(-Delta Delta C(T)) Method. Methods. 2001;25(4):402–8. Epub 2002/02/16. doi: 10.1006/meth.2001.1262S1046-2023(01)91262-9 [pii]. . [PubMed: 11846609]

30. O'Brien MT, Oakhill JS, Ling NX, Langendorf CG, Hoque A, Dite TA, et al. Impact of Genetic Variation on Human CaMKK2 Regulation by Ca(2+)-Calmodulin and Multisite Phosphorylation. Sci Rep. 2017;7:43264. Epub 2017/02/24. doi: 10.1038/srep43264. [PubMed: 28230171]

31. Green MF, Scott JW, Steel R, Oakhill JS, Kemp BE, Means AR. Ca2+/Calmodulin-dependent protein kinase kinase beta is regulated by multisite phosphorylation. J Biol Chem. 2011;286(32):28066–79. Epub 2011/06/15. doi: 10.1074/jbc.M111.251504. [PubMed: 21669867]
32. Tokumitsu H, Hatano N, Fujimoto T, Yurimoto S, Kobayashi R. Generation of Autonomous Activity of Ca2+/Calmodulin-Dependent Protein Kinase Kinase β by Autophosphorylation. Biochemistry. 2011;50(38):8193–201. doi: 10.1021/bi201005g. [PubMed: 21859090]
33. Bland JM, Altman DG. Multiple significance tests: the Bonferroni method. Bmj. 1995;310(6973):170. Epub 1995/01/21. doi: 10.1136/bmj.310.6973.170. [PubMed: 7833759]
34. Tokumitsu H, Iwabu M, Ishikawa Y, Kobayashi R. Differential regulatory mechanism of Ca2+/calmodulin-dependent protein kinase kinase isoforms. Biochemistry. 2001;40(46):13925–32. Epub 2001/11/14. doi: 10.1021/bi010863k. [PubMed: 11705382]
35. Green MF, Scott JW, Steel R, Oakhill JS, Kemp BE, Means AR. Ca2+/Calmodulin-dependent Protein Kinase Kinase β Is Regulated by Multisite Phosphorylation*. Journal of Biological Chemistry. 2011;286(32):28066–79. doi: 10.1074/jbc.M111.251504.
36. Zhang H, Cai D, Bai X. Macrophages regulate the progression of osteoarthritis. Osteoarthritis and cartilage. 2020;28(5):555–61. Epub 2020/01/27. doi: 10.1016/j.joca.2020.01.007. [PubMed: 31982565]
37. Kennedy A, Fearon U, Veale D, Godson C. Macrophages in Synovial Inflammation. Frontiers in Immunology. 2011;2(52). doi: 10.3389/fimmu.2011.00052.
38. Goldring MB, Goldring SR. Osteoarthritis. J Cell Physiol. 2007;213(3):626–34. doi: 10.1002/jcp.21258. [PubMed: 17786965]
39. Lin H-H, Faunce DE, Stacey M, Terajewicz A, Nakamura T, Zhang-Hoover J, et al. The macrophage F4/80 receptor is required for the induction of antigen-specific efferent regulatory T cells in peripheral tolerance. The Journal of Experimental Medicine. 2005;201(10):1615–25. doi: 10.1084/jem.20042307. [PubMed: 15883173]
40. Kapoor M, Martel-Pelletier J, Lajeunesse D, Pelletier JP, Fahmi H. Role of proinflammatory cytokines in the pathophysiology of osteoarthritis. Nat Rev Rheumatol. 2011;7(1):33–42. Epub 2010/12/02. doi: nrrheum.2010.196 [pii] 10.1038/nrrheum.2010.196. [PubMed: 21119608]
41. Salvat C, Pigenet A, Humbert L, Berenbaum F, Thirion S. Immature murine articular chondrocytes in primary culture: a new tool for investigating cartilage. Osteoarthritis and cartilage. 2005;13(3):243–9. doi: 10.1016/j.joca.2004.11.008. [PubMed: 15727891]
42. Akeson G, Malemud CJ. A Role for Soluble IL-6 Receptor in Osteoarthritis. J Funct Morphol Kinesiol. 2017;2(3):27. Epub 2017/08/02. doi: 10.3390/jfmk2030027. [PubMed: 29276788]
43. Wiegertjes R, van de Loo FAJ, Blaney Davidson EN. A roadmap to target interleukin-6 in osteoarthritis. Rheumatology. 2020;59(10):2681–94. doi: 10.1093/rheumatology/keaa248. [PubMed: 32691066]
44. Sherwood JC, Bertrand J, Eldridge SE, Dell'Accio F. Cellular and molecular mechanisms of cartilage damage and repair. Drug Discovery Today. 2014;19(8):1172–7. doi: 10.1016/j.drudis.2014.05.014. [PubMed: 24880104]
45. Latourte A, Cherifi C, Maillet J, Ea HK, Bouaziz W, Funck-Brentano T, et al. Systemic inhibition of IL-6/Stat3 signalling protects against experimental osteoarthritis. Ann Rheum Dis. 2017;76(4):748–55. Epub 2016/11/01. doi: 10.1136/annrheumdis-2016-209757. [PubMed: 27789465]
46. Green MF, Anderson KA, Means AR. Characterization of the CaMKKbeta-AMPK signaling complex. Cellular signalling. 2011;23(12):2005–12. Epub 2011/08/03. doi: 10.1016/j.cellsig.2011.07.014. [PubMed: 21807092]
47. Terkeltaub R, Yang B, Lotz M, Liu-Bryan R. Chondrocyte AMP-activated protein kinase activity suppresses matrix degradation responses to proinflammatory cytokines interleukin-1β and tumor necrosis factor a. Arthritis and rheumatism. 2011;63(7):1928–37. doi: 10.1002/art.30333. [PubMed: 21400477]
48. Liu-Bryan R. Inflammation and intracellular metabolism: new targets in OA. Osteoarthritis and cartilage. 2015;23(11):1835–42. Epub 2015/11/03. doi: 10.1016/j.joca.2014.12.016. [PubMed: 26521729]

49. Liu-Bryan R, Terkeltaub R. Emerging regulators of the inflammatory process in osteoarthritis. Nat Rev Rheumatol. 2015;11(1):35–44. Epub 2014/10/01. doi: 10.1038/nrrheum.2014.162. [PubMed: 25266449]
50. Loeser RF, Collins JA, Diekman BO. Ageing and the pathogenesis of osteoarthritis. Nat Rev Rheumatol. 2016;12(7):412–20. Epub 2016/05/20. doi: 10.1038/nrrheum.2016.65. [PubMed: 27192932]
51. Fan Z, Söder S, Oehler S, Fundel K, Aigner T. Activation of Interleukin-1 Signaling Cascades in Normal and Osteoarthritic Articular Cartilage. The American Journal of Pathology. 2007;171(3):938–46. doi: 10.2353/ajpath.2007.061083. [PubMed: 17640966]
52. Pal B, Endisha H, Zhang Y, Kapoor M. mTOR: a potential therapeutic target in osteoarthritis? Drugs R D. 2015;15(1):27–36. doi: 10.1007/s40268-015-0082-z.. [PubMed: 25688060]
53. Gwinn DM, Shaw RJ. 3 - AMPK Control of mTOR Signaling and Growth. In: Tamanoi F, Hall MN, editors. The Enzymes. 28: Academic Press; 2010. p. 49–75.
54. Legendre F, Dudhia J, Pujol J-P, Bogdanowicz P. JAK/STAT but Not ERK1/ERK2 Pathway Mediates Interleukin (IL)-6/Soluble IL-6R Down-regulation of Type II Collagen, Aggrecan Core, and Link Protein Transcription in Articular Chondrocytes: ASSOCIATION WITH A DOWN-REGULATION OF SOX9 EXPRESSION*. Journal of Biological Chemistry. 2003;278(5):2903–12. doi: 10.1074/jbc.M110773200.
55. Zhou G, Garofalo S, Mukhopadhyay K, Lefebvre V, Smith CN, Eberspaecher H, et al. A 182 bp fragment of the mouse pro alpha 1(II) collagen gene is sufficient to direct chondrocyte expression in transgenic mice. Journal of cell science. 1995;108(12):3677–84. doi: 10.1242/jcs.108.12.3677. [PubMed: 8719874]
56. Akiyama H, Chaboissier M-C, Martin JF, Schedl A, de Crombrugghe B. The transcription factor Sox9 has essential roles in successive steps of the chondrocyte differentiation pathway and is required for expression of Sox5 and Sox6. Genes & development. 2002;16(21):2813–28. doi: 10.1101/gad.1017802. [PubMed: 12414734]
57. Weigert C, Düfer M, Simon P, Debre E, Runge H, Brodbeck K, et al. Upregulation of IL-6 mRNA by IL-6 in skeletal muscle cells: role of IL-6 mRNA stabilization and Ca2+-dependent mechanisms. American Journal of Physiology-Cell Physiology. 2007;293(3):C1139–C47. doi: 10.1152/ajpcell.00142.2007.. [PubMed: 17615159]
58. Williams JN, Kambrath AV, Patel RB, Kang KS, Mevel E, Li Y, et al. Inhibition of CaMKK2 Enhances Fracture Healing by Stimulating Indian Hedgehog Signaling and Accelerating Endochondral Ossification. Journal of bone and mineral research : the official journal of the American Society for Bone and Mineral Research. 2018. Epub 2018/01/10. doi: 10.1002/jbmr.3379.
59. Chien SY, Huang CY, Tsai CH, Wang SW, Lin YM, Tang CH. Interleukin- 1β induces fibroblast growth factor 2 expression and subsequently promotes endothelial progenitor cell angiogenesis in chondrocytes. Clin Sci (Lond). 2016;130(9):667–81. Epub 2016/01/27. doi: 10.1042/cs20150622. [PubMed: 26811540]

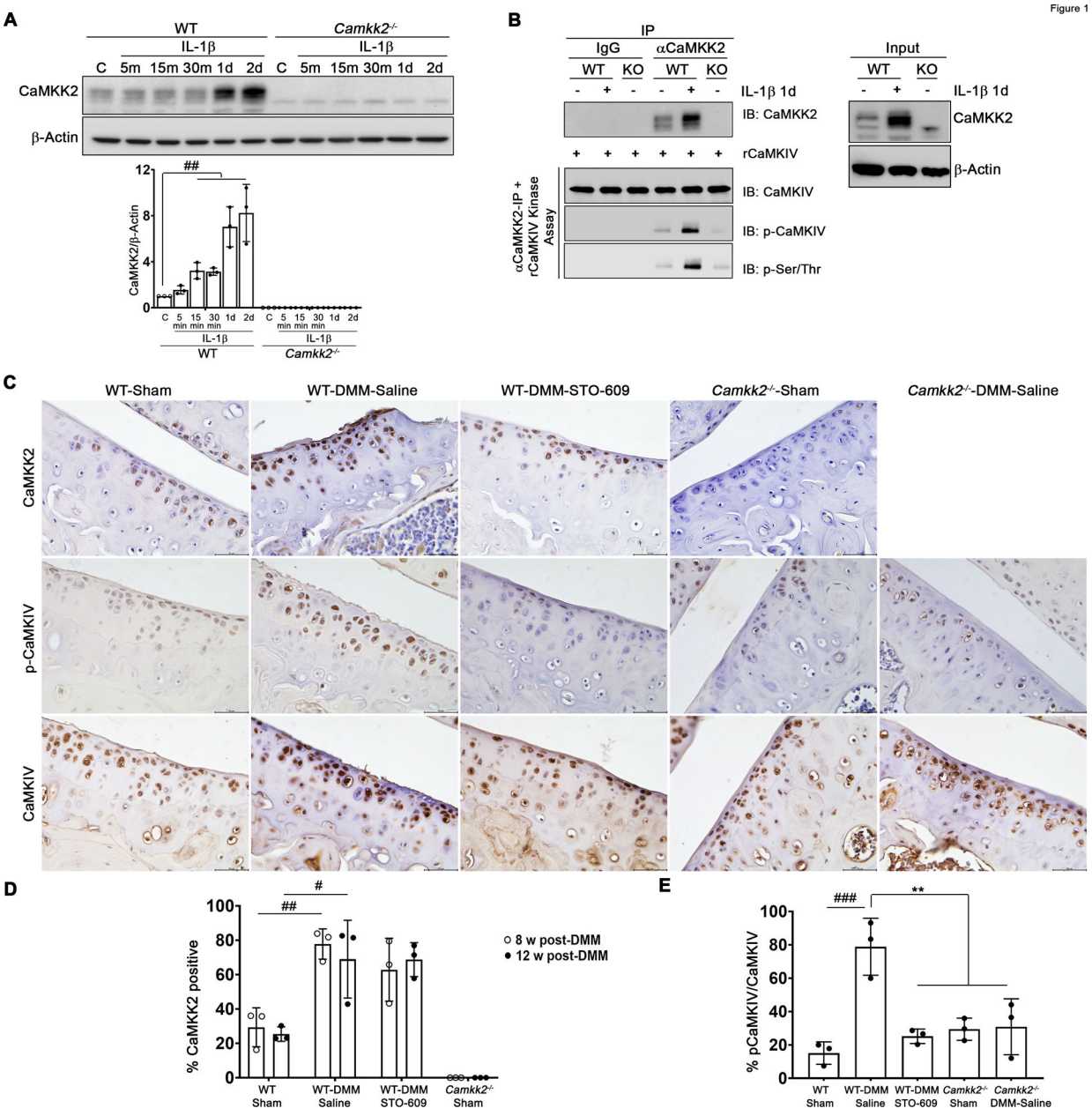

Figure 1. Articular chondrocytes express CaMKK2, and its levels and activity are elevated with OA.

(A) (Top) Immunoblots of cell extracts from WT and *Camkk2*$^{-/-}$ iMACs unstimulated (C) or stimulated with 10 ng/ml of IL-1β for indicated time points, and probed for CaMKK2 and b-Actin. Representative blots from n=3 independent experiments are shown. **(Bottom)** Average signal intensities calculated of CaMKK2 normalized to the respective levels of loading control (Actin) from n=3 blots. **(B)** Immunoblots (IB) of CaMKK2 immunoprecipitation (IP)-kinase assay with recombinant (r) CaMKIV as substrate from indicated samples. Five hundred μg of cell lysis supernatants from WT iMACs treated with PBS or IL-1β (10 ng/ml, 1 day) and untreated *Camkk2*$^{-/-}$ iMACs were incubated with control IgG or αCaMKK2 antibody, and the activity of immunocomplexes tested against

rCaMKIV. About 1/50th of the IP-kinase assays (2 μl/100 μl) were resolved on SDS-PAGE and probed for CaMKK2 and total CaMKIV immunoreactivity in addition to probing for pCaMKIV and p-Ser/Thr immunoreactivity to assess CaMKIV phosphorylation in the IP-kinase assays. Input with 1/100th (5/500 μg) of total protein used in the IP loaded is shown. Representative blots from n=3 independent experiments are shown. **(C)** Representative images (400X) of articular cartilage sections from WT-sham, WT-DMM-saline (OA) or *Camkk2*$^{-/-}$-DMM mice collected at 12 w post-surgery, and probed for immunoreactivity against CaMKK2, phospho (p) CaMKIV and total CaMKIV by IHC. **(D)** Quantification of CaMKK2 IHC and **(E)** quantification of pCaMKIV/total CaMKIV IHC in the indicated genotypes (n=3/cohort). Error bars = standard deviation (SD); *p*-values: $^{\#}$ $p<0.05$; $^{\#\#}$ $p<0.01$, $^{\#\#\#}$ $p<0.001$.

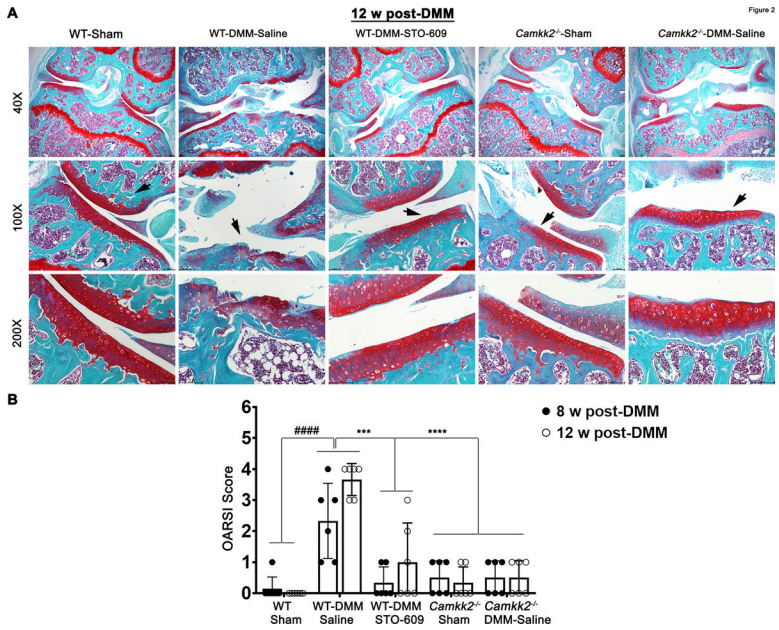

Figure 2. Loss or inhibition of CaMKK2 protects from cartilage degradation associated with OA

(A) Representative images (40X - top row, 100X - middle row and 200X - bottom row) of cartilage sections stained with safranin O fast green at 12 w post-surgery from WT-sham, WT-DMM-saline, WT- DMM-STO-609, *Camkk2*$^{-/-}$-sham or *Camkk2*$^{-/-}$-DMM. Black arrowheads represent articular cartilage. **(B)** OA severity assessed using the histological OARSI scoring system at 8 and 12 w post-surgery (n=6 per group). Error bars = SD; *p*-values: $^{\#\#\#\#}$ ***p***<0.0001 compared to WT-sham, *** $p < 0.001$ and ****$p < 0.0001$ compared to WT-DMM-saline.

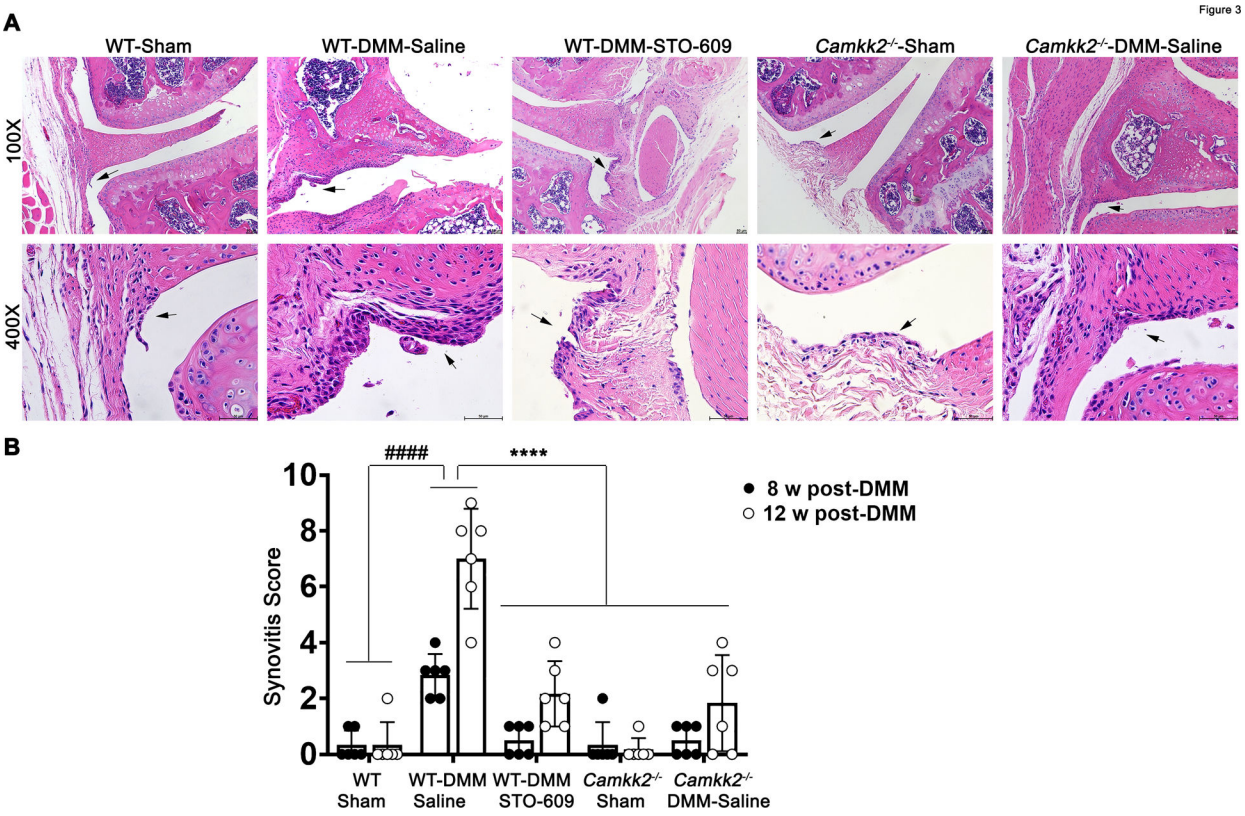

Figure 3. OA-associated synovitis is abrogated in STO-609-treated DMM-WT and *Camkk2*$^{-/-}$ mice.

(A) Images of H&E stained sections (100X and 400X) of the synovium from indicated groups (representative of n=6/group). **(B)** Histological synovitis score at 8 and 12 w post-surgery in WT and *Camkk2*$^{-/-}$ mice; n=6/group. Error bars = SD; *p*-values: #### $p < 0.0001$, compared to WT-sham, and **** $p < 0.0001$ compared to WT-DMM-saline.

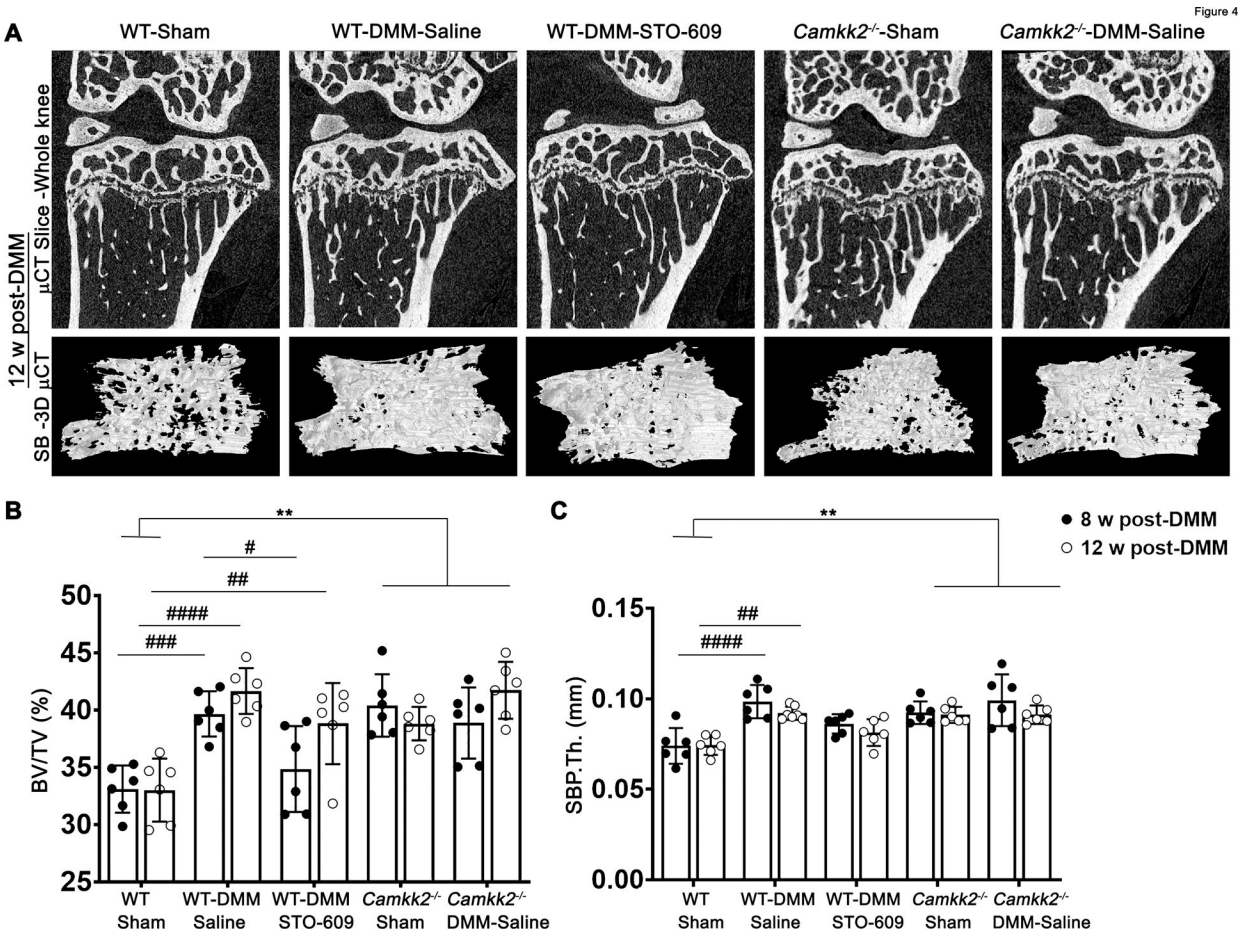

Figure 4. CaMKK2 inhibition protects against DMM-associated alterations to subchondral bone.

(A) 3D-pCT image slice of whole knee joints and image reconstruction of SB (representatives; coronal view) of WT-sham, WT-DMM-saline, WT-DMM-STO-609, *Camkk2*$^{-/-}$-sham or *Camkk2*$^{-/-}$-DMM mice at 12 w post-surgery. **(B and C)** Mean percent bone volume of SB (BV/TV) and SBP thickness (SBP.Th.) analyzed at 8 and 12 w post-surgery from µCT images. Error bars = SD; *p*-values: #### $p < 0.0001$, ### $p<0.001$, ## $p<0.01$, # $p<0.05$ compared to WT-sham, ** $p < 0.01$compared to WT-DMM-saline.

Figure 5

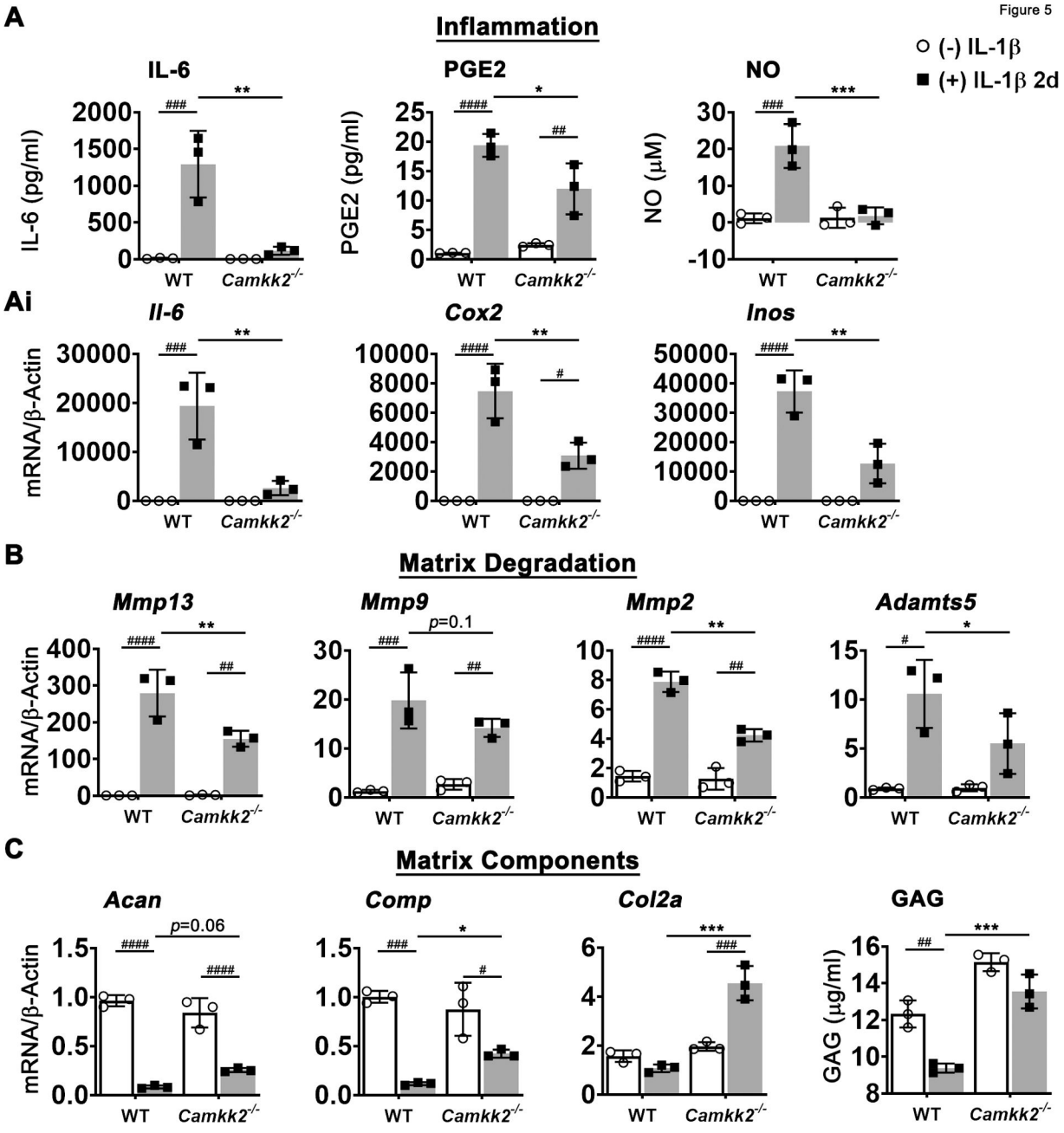

Figure 5. Loss of CaMKK2 in articular chondrocytes attenuates inflammatory and catabolic responses to IL-ip while preserving anabolic responses.

(A) IL-6, NO, and PGE_2 levels measured in the culture media from WT and *Camkk2*$^{-/-}$ iMACs after IL-1β stimulation (10 ng/ml, 2 days). **(Ai)** *Inos, Cox2*, and *Il-6* mRNA relative to *β-Actin* in WT and *Camkk2*$^{-/-}$ iMACs stimulated with IL-1β. **(B)** Levels of *Mmp2, Mmp9, Mmp13*, and *Adamts5* mRNA relative to *β-Actin* from WT and *Camkk2*$^{-/-}$ chondrocytes after IL-1β stimulation. **(C)** Normalized levels of ECM components *Acan, Comp,* and *Col2a1* mRNA as well as glycosaminoglycan (GAG) content in the culture media as indicated. N=3. Error bars = SD; *p*-values: #### $p< 0.0001$, ### $p<0.001$, ## $p<0.01$,

[#] $p<0.05$ for comparisons within genotype; and * $p < 0.05$, ** $p < 0.01$, *** $p < 0.001$ for comparisons between genotypes.

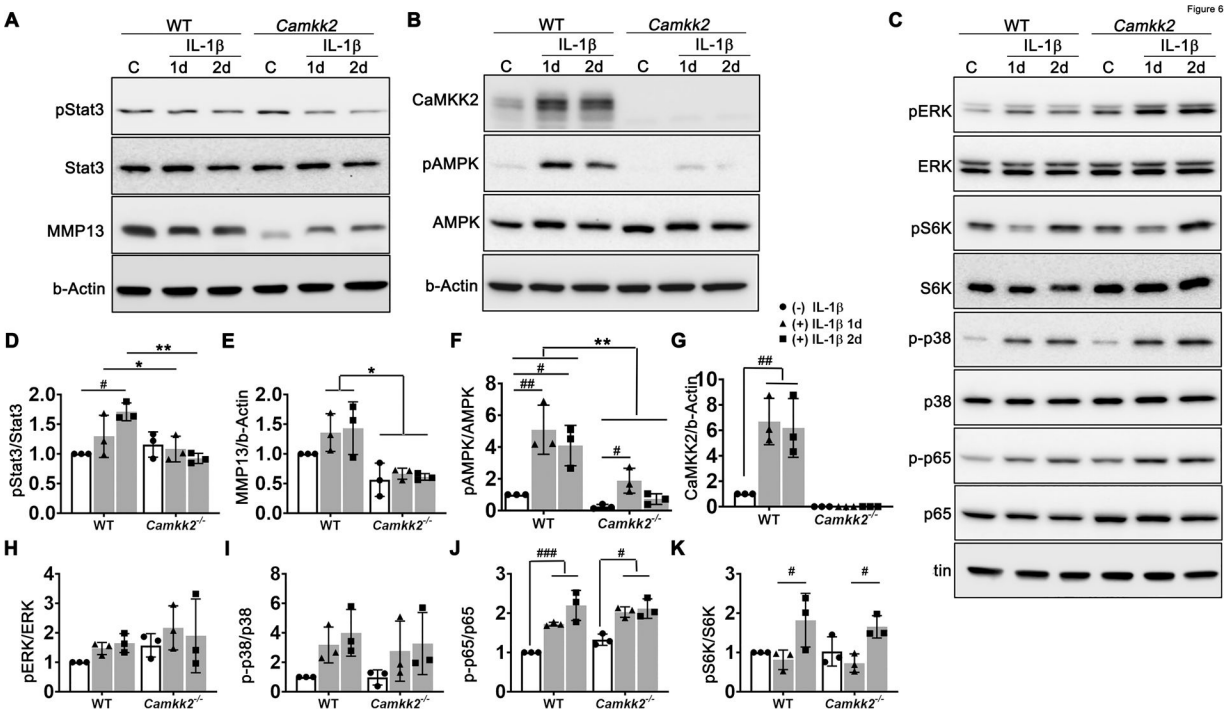

Figure 6. CaMKK2 modulates IL-1β-mediated activation of Stat3-MMP13 and AMPK in chondrocytes.

(A-C) Immunoblots of cell extracts from WT and *Camkk2*$^{-/-}$ iMACs unstimulated (C) or stimulated with 10 ng/ml of IL-1β for 1 or 2 days, and probed for **(A)** phospho- and total Stat3, MMP-13 and b-Actin; **(B)** CaMKK2, phospho- and total AMPK and b-Actin; and **(C)** phospho and total ERK, S6 Kinase, p38 and p65 as well as b-Actin. **(D-K)** Average signal intensities of the indicated proteins. The ratio of phosphoprotein band intensities over the total levels of the respective proteins (Stat3, AMPK, ERK, S6K, p38 MAPK and p65 (Rel1/NF-κB) and/or total protein band intensities over the levels of b-Actin (CaMKK2 and MMP-13) are shown. Representative blots and quantification from n=3 independent experiments are shown. Error bars = SD; *p*-values$^{###}$ $p<0.001$, $^{##}$ $p<0.01$, $^{#}$ $p<0.05$ for comparisons within genotype; * $p < 0.05$, ** $p < 0.01$ for comparisons between genotypes.

Table 1.

List of primary antibodies used in this study per application:

Primary Antibody	Vendor	Catalogue Number	Antibody Dilution	Application
Rabbit anti-CaMKK2-NT	Abcam, Cambridge, UK	ab124096	1:100	IHC
Rabbit anti-CaMKK2-NT	US Biological, Salem, MA	033168	1:100	IHC
F 4/80	BioRad, Hercules, CA	MCA497GA	1:250	IHC
Type II Collagen	Thermo Fisher, Waltham, MA	MA512789	1:100	IHC
MMP-13	Thermo Fisher	MA514238	1:100	IHC
mouse anti-CaMKIV	BD, Franklin Lakes, NJ	610275	1:100 1:1000	IHC IB
Rabbit anti-phospho CaMKIV (Thr196, Thr200)	Invitrogen, Waltham, MA	PA5–105011	1:100 1:1000	IHC IB
Rabbit anti-Phospho - (Ser/Thr) Phe antibody	Abcam	Ab17464	1:1000	IB
mouse anti-CaMKK	BD	610544	1:1000	IB
rabbit anti-p-AMPKa (Thr172)	Cell signaling, Danvers, MA	2535	1:1000	IB
rabbit anti-AMPKa	Cell signaling	5832	1:1000	IB
rabbit anti-p-p38 (Thr180/Tyr182)	Cell signaling	9211	1:1000	IB
rabbit anti-p38	Cell signaling	9212	1:1000	IB
rabbit anti-p-NF-κB p65(Ser536)	Cell signaling	3033	1:1000	IB
rabbit anti-NF-κB p65	Cell signaling	8242	1:1000	IB
rabbit anti-p-ERK (Thr202/Tyr204)	Cell signaling	4370	1:1000	IB
rabbit anti-ERK	Cell signaling	4695	1:1000	IB
rabbit anti-p-S6 (Ser235/236)	Cell signaling	4858	1:1000	IB
rabbit anti-S6	Cell signaling	2217	1:1000	IB
rabbit anti-p-Stat3(Tyr705)	Cell signaling	9131	1:1000	IB
rabbit anti-Stat3	Cell signaling	9132	1:1000	IB
rabbit anti-MMP13	Abcam	ab39012	1:1000	IB
Mouse anti-b-Actin	Sigma, St. Louis, MO	A1978	1:10,000	IB

IHC – Immunohistochemistry; IB – Immunoblotting

Table 2.

List of qRT-PCR primers used in this study:

Target	Forward primer: 5'–3'	Reverse primer: 5'–3'	AT
Col2a1	AT CTT GCCGCAT CTGTGT GT	CTCCTTTCTGCCCCTTTGGC	55°C
Acan	GGT CACTGTT ACCGCCACTT	CCCCTTCGATAGTCCTGTCA	55°C
Comp	TGCGACGACGACATAGATGG	ACATCCCTCTGGTCTGGGTT	55°C
Mmp2	CCTGCCCACCCAATGGTAAA	AGAAGTAGCTATGACCACCACCC	55°C
Mmp9	ACTCACACGACATCTTCCAG	AGAAGGAGCCCTAGTTCAAG	55°C
Mmp13	GACCCACAGATGAGCACAGA	ATGTAAGGCCACCTCCACTG	55°C
Adamts5	CCTGCCCACCCAATGGTAAA	GTCCTCGGACACACACAGAG	55°C
Cox2	TGAGTACCGCAAACGCTTCT	ACGAGGTTTTTCCACCAGCA	55°C
Il-6	TGAGAAAAGAGTTGTGCAATGG	TCTCTCTGAAGGACTCTGGCT	55°C
Inos	TTTGTGCGAAGTGTCAGTGG	CAAACACCAAGCTCATGCGG	55°C

AT – Annealing Temperature